International Journal of Nanoelectronics and Materials

In Press, Accepted Manuscript – Note to user

Synthesis of Silica-coated Iron Oxide Nanoparticles: Effect of Particle Sizes and Silica Coating

Zhe Jia Ng[1], Yeit Haan Teow[1,2*], Abdul Wahab Mohammad[1,2], Kah Chun Ho[1,2], and Swee Pin Yeap[3]

[1]Department of Chemical and Process Engineering, Faculty of Engineering and Built Environment, Universiti Kebangsaan Malaysia, 43600 UKM Bangi, Selangor Darul Ehsan, Malaysia.
[2]Research Centre for Sustainable Process Technology (CESPRO), Universiti Kebangsaan Malaysia, 43600 UKM Bangi, Selangor Darul Ehsan, Malaysia.
[3]Department of Chemical & Petroleum Engineering, Faculty of Engineering, Technology & Built Environment, UCSI University, 56000 Cheras, Kuala Lumpur, Malaysia.

Received 17 August 2020, Revised 25 Aug 2020, Accepted 26 Aug 2020

ABSTRACT

The development of magnetic nanoparticles has gained attention in the field of wastewater treatment but faced several challenges including instability and extremely sensitive to oxidation. Hence, surface modification was generally used as by coating a layer of polymer on the surface of magnetic nanoparticles. The present study focuses on the synthesis and characterization of silica-coated iron oxide nanoparticles (IONPs) with different concentrations of IONPs and tetraethyl orthosilicate (TEOS). The IONPs were first synthesized by the co-precipitation method followed by the surface modification of silica on the IONPs through the modified Stober process. The effect of IONPs concentration (1000 mg/L to 10000 mg/L) and TEOS concentration (1 wt% to 10 wt%) was studied through the hydrodynamic particle size and colloidal stability of silica-coated IONPs. The results showed that the IONPs have an average hydrodynamic particle size of 317.53 nm, and zeta potential of -14.33 mV. Besides, it was observed that the increase in concentration of TEOS and decrease in concentration of IONPs lead to nanoparticle agglomeration, thus resulting in large particle size. The optimized concentration of IONPS and TEOS is 5500 mg/L and 5.5 wt%, producing silica-coated IONPS with the smallest particle size (228.23 nm) and high colloidal stability (-20.93 mV).

Keywords: Silica-coated iron oxide nanoparticles, Tetraethyl orthosilicate, Iron oxide nanoparticles

1. INTRODUCTION

In the past decades, water pollution had raised public concern especially in developing countries. Several factors have influenced the increase in water pollution level and they mainly include global population growth, rapid industrialization, and over-exploitation of natural resources [1, 2]. Due to the negative impacts of water pollution, the wastewater needs to be treated before discharged into the surface water streams. Conventional wastewater treatment such as chemical precipitation [3, 4], chemical coagulation [5], ion exchange [6, 7], electrochemical [8, 9], membrane filtration [10, 11], and biological treatment [12, 13] had been employed for the removal of pollutants in wastewater. However, those conventional treatments were found to have some limitations on the application. The chemical treatment such as chemical precipitation, chemical coagulation, ion exchange, and electrochemical method has been cited to have high capital and operating costs, as well as a large amount of sludge is produced. Additionally, physical

treatment such as membrane filtration also faced some challenges as the membrane fouling will restrict the removal efficiency of pollutants.

Recently, much literature reveals that the physicochemical method using the adsorption process showed its advantages in the removal of pollutants including simple operation, cost-effectiveness, and high adsorbent efficiency. The advancement in nanotechnology had turned up to the development of magnetic nanoparticles in wastewater treatment [14]. The magnetic nanoparticles have responded very well to a high surface area, high adsorption capacity, and easy separation due to magnetic property [15]. Cheng et al. [16] studied the feasibility of iron oxide nanoparticles (IONPs) as the alternative replacement for conventional adsorbents. The results showed that the IONPs had successfully removed more than 90 % of lead ions (Pb^{2+}) at a concentration of 50 mg/L of Pb^{2+} within 15 minutes. Furthermore, Jin et al. [17] also reported that the IONPs reached a maximum adsorption capacity for chromium (VI) (Cr^{6+}) and copper (II) (Cu^{2+}) at 8.67 mg/g and 18.61 mg/g in the mixture of 80 mg/dm^3 Cr^{6+} and Cu^{2+}. The IONPs had provided a promising performance in the pollutants removal and could be easily separated under the magnetic field. Subsequently, surface modification on the IONPS was studied extensively to improve their surface properties such as charge density, functionality, biocompatibility, and colloidal stability [18]. Typically, mesoporous silica is widely used as the protection layer of IONPs to prevent oxidation together with the improvement in the adsorption capacity. Nicola et al. [19] had used the tetraethyl orthosilicate (TEOS) as the silica source for the surface modification of IONPs to remove the Pb^{2+} from aqueous solution. The result showed that the silica-coated IONPs presented a maximum adsorption capacity of 14.9 mg/g. Other than that, Unob et al. [20] utilized the waste silica in the surface modification of IONPs to obtain an adsorbent for the removal of lead (II), copper (II), cadmium (II), and nickel (II). The adsorbent could achieve the removal efficiencies of heavy metals ranging between 62 to 89 %. This further proved that the silica-coated IONPs have a good performance in the pollutants removal. Moreover, the silica layer also can prevent the agglomeration of IONPs in solution without affecting the magnetic strength, thus enhance the dispensability in a suspension medium [15].

Ongoing through the published information, it is known that the IONPs and TEOS concentration had played an important role in the removal efficiency of the pollutants. As reveal from Li et al. [21], the magnetic strength of silica-coated IONPs reduces correspondingly upon the increase in TEOS concentration, thus making the mass proportion of IONPs smaller. The thick silica layer that hinders the magnetic strength may slow down the magnetic separation process and result in ineffective adsorbent recovery. Similar to IONPs concentration, the increase in IONPs concentration can lead to the formation of large particle size. As reported by Yean et al. [22], the magnetite nanoparticles with smaller particles size have a better adsorption capacity for As(III) and As(V) as compared to large magnetite nanoparticles. This is due to the small magnetite nanoparticles have a large adsorption surface area, hence exposed more adsorption sites to the heavy metal ions.

Hence, this paper aimed to study on the effect of TEOS and IONPs concentration in the synthesis of silica-coated IONPs. In this paper, the silica-coated IONPs with different concentrations of IONPs and TEOS were synthesized in two steps. First, the IONPs were prepared by the co-precipitation method followed by coating with a layer of silica through a modified Stober process. The silica-coated IONPs were then characterized through Fourier transform infrared (FTIR) spectroscopy, hydrodynamic particle size, particle size distribution, and zeta potential.

2. MATERIAL AND METHODS

2.1 Materials

Absolute ethanol (C_2H_5OH) (purity: 99.8%), ammonia solution ($NH_3•H_2O$) (purity: 25%), and sodium hydroxide (NaOH) were supplied by Systerm, Malaysia. TEOS (purity: 98%), iron (III) chloride ($FeCl_3$) (purity: 98%), iron (II) chloride tetrahydrate ($FeCl_2•4H_2O$) (purity: 99%) were purchased from Acros Organics, USA. On the other hand, hydrochloric acid (HCl) (purity: 32%) was obtained from Avantor, USA, respectively. All chemicals in this study were analytical grade and used as received without further purification.

2.2 Synthesis of Silica-coated IONPs

2.2.1 Synthesis of IONPs

IONPs were synthesized through the co-precipitation method [23]. Prior to the synthesis of IONPs, HCl was diluted to 0.5 M and deoxygenated by bubbling it with nitrogen gas for 30 minutes. It was followed by the addition of 6.5 g of $FeCl_3$ and 5.56 g of $FeCl_2•4H_2O$ into the 50 mL of 0.5 M HCl [24]. The molar ratio of $FeCl_3$ to $FeCl_2$ was kept at 2:1. Next, the mixture was sonicated in an ultrasonic bath, WUC-A03H (Daihan, Korea) for 30 minutes. It was then transferred into a 1 L three-necked round bottom flask and bubbling with nitrogen gas for 30 minutes. Meanwhile, the mixture in the three-necked round bottom flask was heated to 80 ^{0}C under continuous stirring at 500 rpm [25]. Once the mixture in three-necked round bottom flask reached 80 ^{0}C, 500 mL of 1.5 M NaOH was added drop-by-drop into the mixture. The mixture was stirred continuously for 15 minutes after adding NaOH. The black precipitate, IONPs was formed after the process. The precipitate was then isolated with a neodymium magnet and washed with reverse osmosis (RO) water followed by absolute C_2H_5OH until reach pH 7. The collected powder was further dried in a freeze dryer at -45 ^{0}C for 1 day. The experimental set up for the synthesis of IONPs was shown in Figure 1.

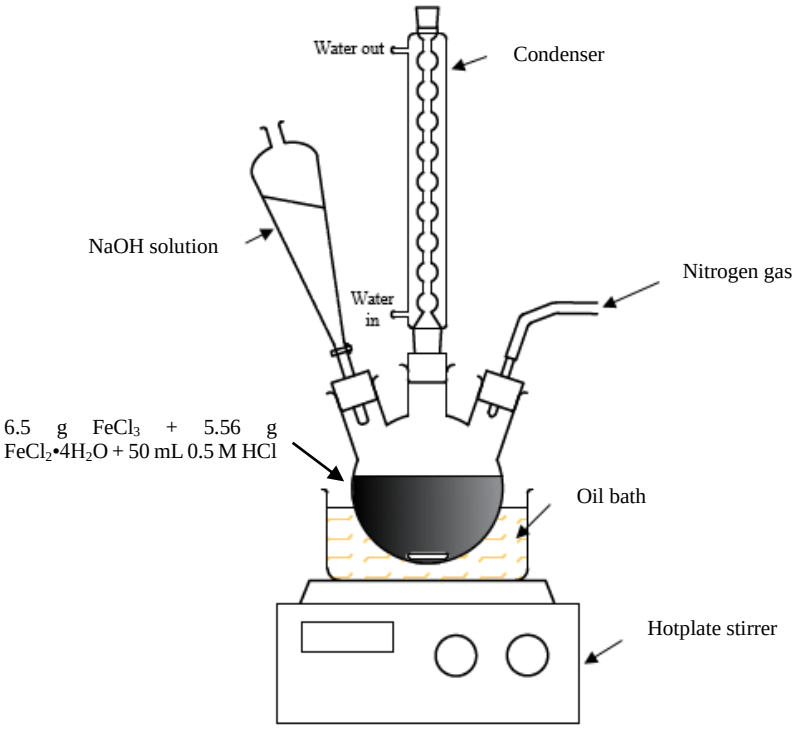

Figure 1. Experimental set-up for the synthesis of IONPs.

2.2.2 Synthesis of Silica-coated IONPs

Silica-coated IONPs were synthesized through a modified Stober process [26]. Firstly, IONPs (1000-10000 mg/L) were added into the ethanol-RO water solution with a volume ratio of 10:1 [27]. The mixture was then sonicated with an ultrasonic bath (Daihan, Korea) for 15 minutes. Next, the TEOS with different concentrations (1-10 wt%) was added to the mixture [28]. Ammonia solution was added slowly into the mixture with continuous stirring and pH was adjusted to 11. The reaction was continued at room temperature for 12 hours under vigorous stirring at 400 rpm. When the reaction is completed, the silica-coated IONPs was isolated by a neodymium magnet and washed with RO water followed by absolute C_2H_5OH until the supernatant turned neutral. The collected powder was further dried in freeze dryer at -45 ^{0}C for 1 day.

2.2.3 Formulation of synthesized nanoparticles

As shown in Table 1, different concentrations of IONPs and TEOS were used to prepare the synthesis of silica-coated IONPs. To determine the effect of particle sizes and silica-coating, the concentration of IONPs in the modified Stober process varied in the range of 1000 mg/L to 10000 mg/L. Whereas, the concentration of TEOS was manipulated in the range of 1 wt% to 10 wt% [28]. The effect of particle sizes and silica coating was evaluated based on the achieved hydrodynamic particle size measured using Malvern Nano ZS light-scattering (Malvern Instrument Ltd., UK).

Table 1 The formulation of silica-coated IONPs in the modified Stober process

Sample nomenclature	Concentration of IONPs (mg/L)	Concentration of TEOS (wt%)
1	1000.000	5.500
2	2824.284	8.176
3	2824.284	2.824
4	2824.284	2.824
5	2824.284	8.176
6	5500.000	10.000
7	5500.000	5.500
8	5500.000	5.500
9	5500.000	5.500
10	5500.000	5.500
11	5500.000	1.000
12	5500.000	5.500
13	5500.000	5.500
14	5500.000	5.500
15	5500.000	5.500
16	8175.716	8.176
17	8175.716	2.824

18	8175.716	8.176
19	8175.716	2.824
20	10000.000	5.500

2.3 Characterization of Nanoparticles

2.3.1 Functional Groups

The functional groups that existed on the synthesized nanoparticles were ascertained using FTIR spectroscopy, Nicolet 6700 (Thermo Fisher Scientific, USA). The FTIR spectroscopy was coupled with a diamond crystal and operated at a wavelength ranging from 400 cm^{-1} to 4000 cm^{-1}. Equal pressure was applied to the synthesized nanoparticles to avoid any difference caused by pressure or penetration depth.

2.3.2 Hydrodynamic Particle Size and Particle Size Distribution

The hydrodynamic particle size and particle size distribution of the synthesized nanoparticles were measured by dynamic light scattering (DLS) method with the use of Malvern Nano ZS light-scattering (Malvern Instrument Ltd., UK). The nanoparticles were first prepared in RO water with the concentration of 10 mg/mL at pH 7. The nanoparticle suspension was then sonicated for 15 minutes prior to analysis. The nanoparticle suspension was illuminated with a laser beam at 630 nm wavelength. The light scattering detection angle was set at 173^0. The autocorrelation function of the photocurrent was obtained every 10 seconds and each run consists of 15 acquisitions. The z-averaged hydrodynamic mean diameter (dz) and distribution profile of the nanoparticle suspension was calculated using Malvern Zetasizer software version 7.11. Each nanoparticles suspension was measured 3 times and the average hydrodynamic particle size value was reported.

2.3.3 Zeta Potential

The zeta potential of the synthesized nanoparticles was determined by laser Doppler velocimetry (LDV) technique with the aid of Malvern Nano ZS light-scattering (Malvern Instrument Ltd., UK). The nanoparticles were first prepared in RO water with the concentration of 10 mg/mL at pH 7. Then, the nanoparticles were sonicated for 15 minutes prior to analysis. Next, 2 mL of nanoparticle suspension was injected into the folded capillary zeta cell (DTS 1070). The light scattering detection angle was set at 90^0 and an electric field with a voltage of 4.96 ± 0.05 V was applied to the nanoparticles suspension sample. Each nanoparticles suspension was measured 3 times and the average zeta potential value was reported.

3. RESULTS AND DISCUSSION

3.1 Physical Observation of IONPS and Silica-coated IONPS

Figure 2(a) and Figure 2(b) show the images of IONPS suspension in RO water. It was observed that deep black monophasic dispersion of IONPS was obtained after co-precipitation process. Once the neodymium magnet was brought near to the dispersion, the IONPS started to attract each other and form aggregates which become visible at the wall near to the neodymium magnet. This confirms that IONPS with strong magnetic properties were obtained. Besides, it was also

observed that silica-coated IONPS (Sample 5) (Figure 2(d)) with IONPs concentration of 2824.284 mg/L and TEOS concentration of 8.176 wt% appeared to be brownish as compared with black pristine IONPS (Figure 2(c)). This is due to the nucleation of formed silica on the surfaces of IONPS based on the hydrolysis and polycondensation of TEOS in the presence of water and alkaline media (ammonia). The silica coating layer is expected to improve the surface charge and reactivity of IONPS.

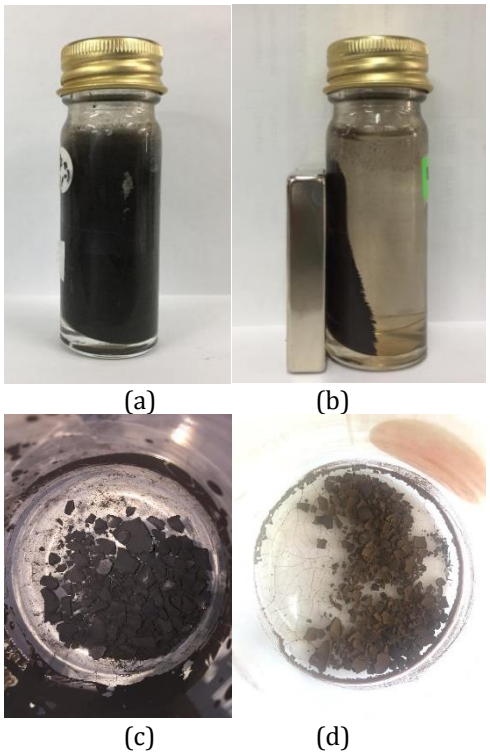

(a) (b)

(c) (d)

Figure 2. Image of (a) IONPs in suspension, (b) IONPs attracted to neodymium magnet, (c) freeze-dried IONPs, and (d) freeze-dried silica-coated IONPs (Sample 5).

3.2 Functional Group

Figure 3 presents the FTIR spectra of IONPs and silica-coated IONPs represented by Sample 7. As shown in Fig 4(a), a wide peak was observed around 570 cm^{-1} corresponds to the stretching vibration of the Fe-O bond and no additional peaks were seen [29]. This was due to the large particle size of IONPs would affect the intensity and area of IR and caused the other peaks showed insignificantly [30, 31]. The adsorption band at 570 cm^{-1} further proved that the magnetite IONPs with the tetrahedral and octahedral sites were successfully synthesized [32].

Compared to IONPs, the Fe-O bond also detected around 580 cm^{-1} in the silica-coated IONPs (Sample 7). The characteristic peaks at 1082 cm^{-1} and 455 cm^{-1} were assigned to the symmetric and asymmetric stretching vibration of Si-O-Si by the hydrolysis and condensation reaction of silicone alkoxides [33]. These vibrations are believed to have strong IR absorption, which is matched with their appearance in the spectra. The weak peak around 960 cm^{-1} was attributed to the Si-OH stretching vibration due to the deformation of Si-OH from the incomplete condensation of the TEOS solution. Besides that, two broad peaks have appeared around 3410 cm^{-1} and 1635 cm^{-1} corresponds to –OH bond in the surface water molecules. Since most of the functional groups appear in the spectra of silica-coated IONPs, it is proved that the silica was successfully coated on the surface of IONPs [34].

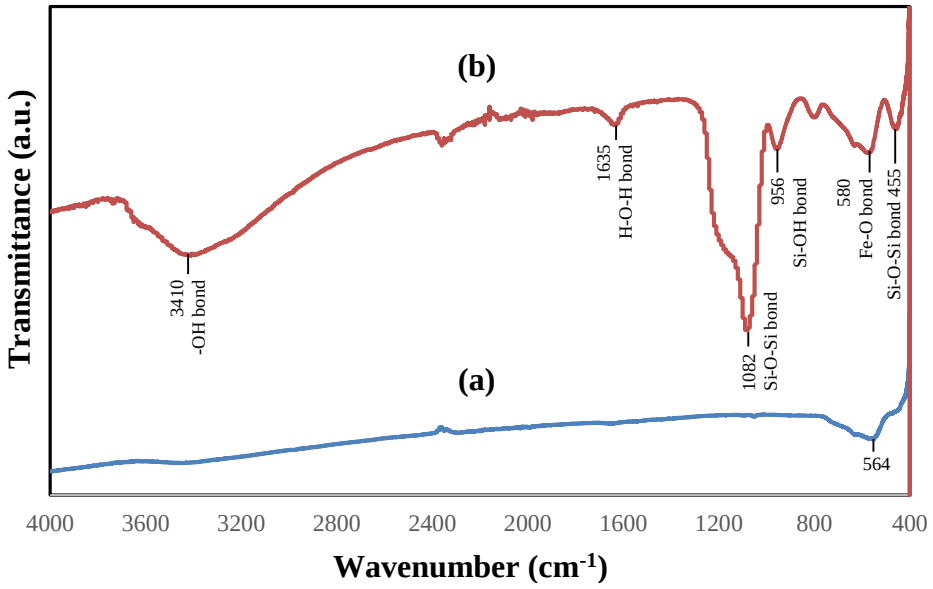

Figure 3. FTIR spectra of nanoparticles (a) IONPs and (b) silica-coated IONPs (Sample 7).

3.3 Hydrodynamic Particle Size and Particle Size Distribution

Figure 4 shows the hydrodynamic particle size for IONPs, Sample 7, Sample 11, and Sample 20. Sample 7, Sample 11, and Sample 20 were discussed here to compare the effect of IONPs and TEOS concentration on the particle size as well as the dispersivity. As shown in Figure 4, the IONPs have an average hydrodynamic particle size of 317.53 nm. The particle size of synthesized IONPs are comparatively larger as compared to other literature works. With the same synthesis method, Behera et al. [35] reported that the particle size of IONPs has detected at a range of 10 nm to 120 nm and a mean particle size of 66 nm. Besides, Maggioni et al. [36] also reported that the synthesized IONPs have a hydrodynamic particle size of 104 nm. This can be explained by the magnetic dipole-dipole attractions between IONPs, the IONPs tend to agglomerate and form large clusters, thus resulting in large particle size. Carter [37] also claimed that the electrostatic interactions and surface tension force between the IONPs contributed to the agglomeration effect in IONPs. Therefore, the surface coating of silica on the IONPs was made to reduce the agglomeration size and on the other hand favor the colloidal stability. Sample 7, 11, and 20 for silica-coated IONPs have the hydrodynamic particle size of 228.23 nm, 314.67 nm, and 493.07 nm respectively. By comparing Sample 7 and IONPs, the surface modification of silica on Sample 7 reduced the agglomeration effect, thus reducing the hydrodynamic particle size. Reddy [38] explained that the surface modification of silica reduced the surface force of hydroxyl groups and prevent the formation of oxygen bridge bonds, thereby minimize the agglomeration effect. On the other hand, the effect of IONPs concentration in particle size can be observed in Sample 7 and 20. When the IONPs concentration increases from 5500 mg/L to 10000 mg/L, the particle size had increased from 228.23 nm to 493.07 nm, which the particle size had been double up. This is because the TEOS is insufficient to fully coat the IONPs, making the silica coating process incomplete. With this, the magnetic dipole-dipole interaction between uncoated IONPs caused the agglomeration of the nanoparticles and resulting in larger hydrodynamic particle size [33]. For the effect of TEOS, it can be studied in between Samples 7 and 11. When the TEOS concentration decreases from 5.5 wt% to 1.0 wt%, the particle size had increased from 228.23 nm to 314.67 nm. This can be explained by the sufficient concentration of TEOS used in Sample

7. The IONPs were expected to be fully coated, thus reduce the van der Waals force in attracting the nanoparticles.

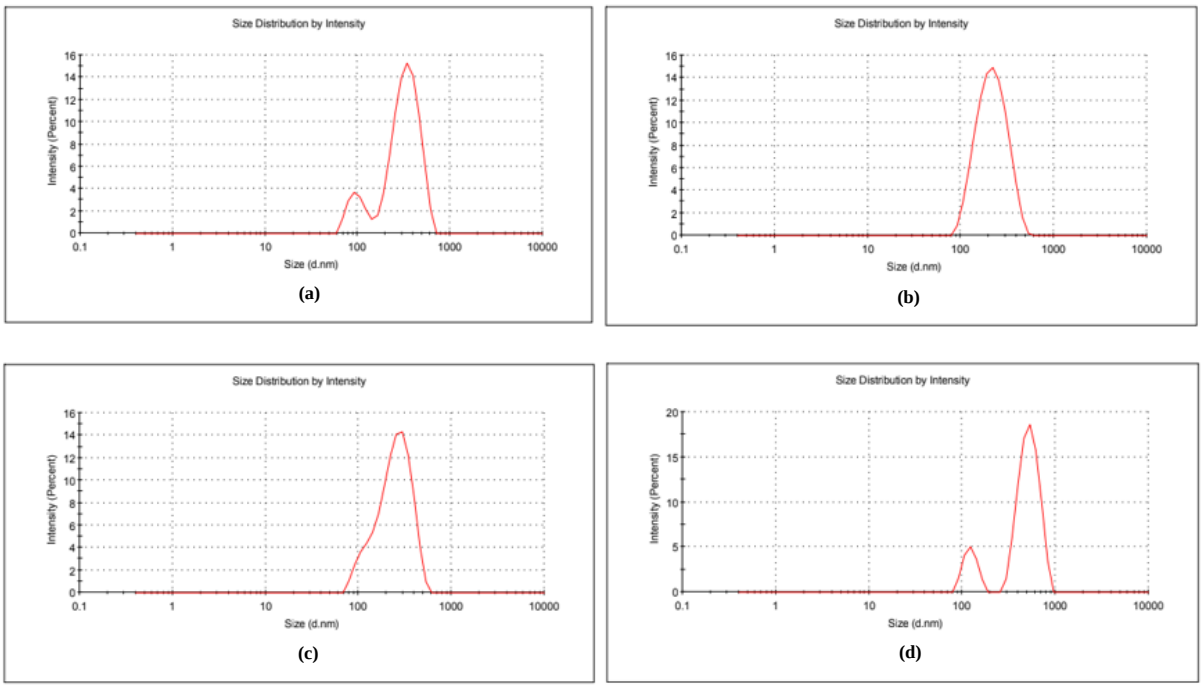

Figure 4. Hydrodynamic particle size for (a) IONPs, (b) Sample 7, (c) Sample 11, and (d) Sample 20.

Table 2 show the particle size distribution for IONPS, Sample 7, Sample 11, and Sample 20. Polydispersity (PDI) index represents the indicator for the particle size distribution with the range from 0.0 to 1.0. Theoretically, the nanoparticle was considered as monodisperse when the PDI index is less than 0.1 whereas the PDI index at the range of 0.1 to 0.2 showed the nanoparticle has a narrow particle size distribution [39]. For the PDI index range from 0.2 to 0.5, the nanoparticle was said to have a moderate dispersity with a narrow particle size distribution whereas the PDI index greater than 0.7 indicates the nanoparticle has very broad particle size distribution. In other words, the PDI index also represents the colloidal stability of nanoparticles in the liquid. As shown in Table 2, the IONPs have an average PDI index of 0.431, which close to the typical PDI index that ranges from 0.1 to 0.4 [40]. The IONPs were expected to have a moderate dispersity with a narrow particle size distribution. Besides, Sample 7, 11, and 20 for silica-coated IONPs have the PDI index of 0.225, 0.499 and 0.431 respectively. A significant comparison can be observed between IONPs and Sample 7. When the silica was modified on the IONPs, the reduction in the PDI index indicates the improvement of dispersivity, thus reduce the agglomeration effect. Moreover, the effect of IONPs concentration in particle size distribution can be observed in Sample 7 and 20. When the IONPs concentration increases from 5500 mg/L to 10000 mg/L, the PDI index had increased significantly as the insufficient TEOS in the surface modification of IONPs. For the effect of TEOS, it can be studied in between Samples 7 and 11. When the TEOS concentration decreases from 5.5 wt% to 1.0 wt%, the PDI index increases as Sample 11 was expected to be coated with incomplete silica and caused insignificant improvement in the agglomeration.

Table 2 PDI index for (a) IONPs, (b) Sample 7, (c) Sample 11, and (d) Sample 20

Sample	PDI index

IONPs	0.431
Sample 7	0.225
Sample 11	0.499
Sample 20	0.431

3.4 Zeta Potential

Figure 5 shows the zeta potential of IONPs and silica-coated IONPS at different concentrations of IONPs and TEOS. In theory, the nanoparticles are considered to have great stability in the suspension when the zeta potential is lower than -30 mV or greater than +30 mV [41]. This is due to the nanoparticles have sufficient electrostatic repulsion force to repel each other, thus avoiding agglomeration to occur [42]. As seen, the IONPs have the zeta potential value of -14.33 mV, which showed the IONPs is unstable in the colloidal stability. This is due to the presence of magnetic property in the IONPs to attract the nearby nanoparticles, shorten the distance between each nanoparticle, thus caused the aggregation or agglomeration process easily to occur [43]. Also, Mokadem et al. [44] reported that the isoelectric point (IEP) of IONPs was found to be around pH 6.45. As the zeta potential of IONPs was close to the IEP, it is expected to have low stability and dispersibility.

For the silica-coated IONPs, Sample 7, 11, and 20 have the zeta potential of -20.93 mV, -15.60 mV, and -23.77 mV respectively. By comparing Sample 7 and IONPs, the surface modification of silica on Sample 7 increased the colloidal stability and dispersivity in the suspension medium, thus increasing the zeta potential. On the other hand, the effect of IONPs concentration in particle size can be observed in Sample 7 and 20. When the IONPs concentration increases from 5500 mg/L to 10000 mg/L, the zeta potential decrease from -20.93 mV to -23.77 mV, which showed a significant improvement in the colloidal stability. However, the magnetic dipole-dipole attraction force is stronger and dominant in the interaction between nanoparticles. Hence, although there is a slight increase in repulsion force between the nanoparticles, agglomeration still exist as it does not able to overcome the magnetic dipole-dipole attraction force [45]. For the effect of TEOS, it can be studied in between Samples 7 and 11. When the TEOS concentration decreases from 5.5 wt% to 1.0 wt%, the zeta potential increases from -20.93mV to -15.60 mV. The increment in the zeta potential also indicates the reduction in the colloidal stability. The insufficient TEOS concentration in Sample 11 limits the surface modification process, hence did not improve much on the colloidal stability.

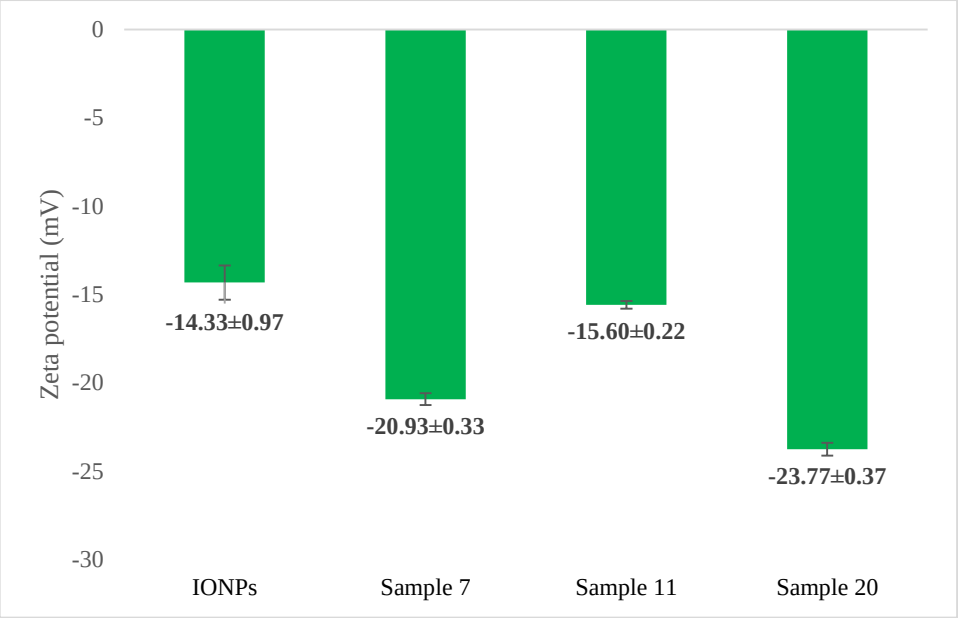

Figure 5. Zeta potential measurement of IONPs and silica-coated IONPs at different concentrations of IONPs and TEOS.

4. CONCLUSION

In summary, magnetite IONPs were synthesized through the co-precipitation method and coated with silica in the modified Stober process. It was found that the concentration of IONPs and TEOS had a significant effect on the particle size and silica layer. This can be observed through the nanoparticle characteristics such as hydrodynamic particle size, zeta potential. For the hydrodynamic particle size, the IONPs, Samples 7, 11, and 20 showed a hydrodynamic particle size of 317.53 nm, 228.23 nm, 314.67 nm, and 493.07 nm respectively. It was realized that Sample 7 has a smaller particle size as compared to the Sample 20 because the TEOS is sufficient to coat at a lower IONPs concentration, thus resulting in a lower particle size. For the effect of TEOS concentration, the particle size showed a reduction in particle size when the concentration of TEOS increased. Besides, the zeta potential analysis demonstrated that the surface coating of IONPs with silica has reduced the agglomeration effect between the synthesized nanoparticles, thus resulted in better dispersity in liquid. It proved that the increase in the concentration of IONPs and TEOS had shown an improvement in colloidal stability. Moreover, the presence of Si-OH and Si-O-Si group in silica-coated IONPs proved that the silica was successfully coated on the surface of magnetite IONPs. Furthermore, this paper suggests the functionalization of chitosan on the silica-coated IONPs in future work. Chitosan functionalization is expected to enhance the performance of nanoparticles in the aspect of adsorption efficiency, adsorption capacity, dispersity, and stability in the wastewater treatment. Optimization of the functionalized silica-coated IONPs is encouraged to conduct in the future for the maximization of the adsorbent performance.

ACKNOWLEDGEMENTS

The authors wish to gratefully acknowledge the financial support of this work by Geran Universiti Penyelidikan (GUP-2017-098) and Dana Modal Insan (MI-2019-017).

REFERENCES

[1] Que, Z.G., J.G.T. Torres, H.P. Vidal, et al., “Application of Silver Nanoparticles for Water Treatment”, Silver Nanoparticles - Fabrication, Characterization and Applications. (2018).
[2] Gehrke, I., A. Geiser, & A. Somborn-Schulz, “Innovations in nanotechnology for water treatment”, Nanotechnology, Science and Applications. **8** (2015) 1–17.
[3] Wu, R., “Removal of heavy metal ions from industrial wastewater based on chemical precipitation method”, Ekoloji. **28** (2019) 2443–2452.
[4] Duarte-Nass, C., K. Rebolledo, T. Valenzuela, et al., “Application of microbe-induced carbonate precipitation for copper removal from copper-enriched waters: Challenges to future industrial application”, Journal of Environmental Management. **256** (2020).
[5] Hargreaves, A.J., P. Vale, J. Whelan, et al., “Impacts of coagulation-flocculation treatment on the size distribution and bioavailability of trace metals (Cu, Pb, Ni, Zn) in municipal wastewater”, Water Research. **128** (2018) 120–128.
[6] Bashir, A., L.A. Malik, S. Ahad, et al., “Removal of heavy metal ions from aqueous system by ion-exchange and biosorption methods”, Environmental Chemistry Letters. **17** (2019) 729–754.
[7] Jiang, J., X.S. Ma, L.Y. Xu, et al., “Applications of chelating resin for heavy metal removal from wastewater”, E-Polymers. **15** (2015) 161–167.
[8] Tran, T.K., K.F. Chiu, C.Y. Lin, & H.J. Leu, “Electrochemical treatment of wastewater: Selectivity of the heavy metals removal process”, International Journal of Hydrogen Energy. **42** (2017) 27741–27748.

[9] Ya, V., N. Martin, Y.H. Chou, et al., "Electrochemical treatment for simultaneous removal of heavy metals and organics from surface finishing wastewater using sacrificial iron anode", Journal of the Taiwan Institute of Chemical Engineers. **83** (2018) 107–114.
[10] Kasim, N. Mohammad, A.W., A.S.R.S., "Retention of heavy metals by nanofiltration membranes: Influence of operating variables", 4th IWA Regional Conference on Membrane Technology. (2014) 3-6 December.
[11] Teow, Y.H., M.S.H. Ghani, W.N.A.W.M. Hamdan, N.A. Rosnan, N.I.M. Mazuki, & K.C. Ho, "Application of Membrane Technology towards The Reusability of Lake Water, Mine Water, and Tube Well Water", Jurnal Kejuruteraan. **29** (2017) 131–137.
[12] Qin, H., T. Hu, Y. Zhai, N. Lu, & J. Aliyeva, *The improved methods of heavy metals removal by biosorbents: A review*, Elsevier, (2020).
[13] Teow, Y.H., N.A.A. Mohamad Zaimi, N.I. Mohamad Mazuki, K.C. Ho, & M. Mohammad Hussein Al Rajabi, "Innovation with The Use of Probiotics as an Eco-friendly Tool for Sewage and Palm Oil Mill Effluent Treatment", International Journal of Nanoelectronics and Materials. **13** (2020) 267–276.
[14] Teow, Y.H., A.W. Mohammad, K.C. Ho, & M. Mohammad Hussein Al Rajabi, "Nualgi Nano Biotechnology Approach to Remediate Eco-Symbiosis for The Conservation of Catchment Lake", International Journal of Nanoelectronics and Materials. **13** (2020) 247–254.
[15] Manyangadze, M., N.H.M. Chikuruwo, T.B. Narsaiah, C.S. Chakra, M. Radhakumari, & G. Danha, "Enhancing adsorption capacity of nano-adsorbents via surface modification: A review", South African Journal of Chemical Engineering. **31** (2020) 25–32.
[16] Cheng, Z., A.L.K. Tan, Y. Tao, D. Shan, K.E. Ting, & X.J. Yin, "Synthesis and characterization of iron oxide nanoparticles and applications in the removal of heavy metals from industrial wastewater", International Journal of Photoenergy. **2012** (2012).
[17] Jin, Z., L. Shuang, H. Meiling, X. Lianqiu, & H. Zhaocong, "Adsorption Properties of Magnetic Magnetite Nanoparticle for Coexistent Cr(VI) and Cu(II) in Mixed Solution", Water(Switzerland). **12** (2020).
[18] Arias, L.S., J.P. Pessan, A.P.M. Vieira, T.M.T. De Lima, A.C.B. Delbem, & D.R. Monteiro, "Iron oxide nanoparticles for biomedical applications: A perspective on synthesis, drugs, antimicrobial activity, and toxicity", Antibiotics. **7** (2018).
[19] Nicola, R., O. Costi, M. Ciopec, A. Negrea, & R. Laz, "Silica-Coated Magnetic Nanocomposites for Pb 2 + Removal from Aqueous Solution", Applied sciences. **10** (2020).
[20] Unob, F., B. Wongsiri, N. Phaeon, M. Puanngam, & J. Shiowatana, "Reuse of waste silica as adsorbent for metal removal by iron oxide modification", **142** (2007) 455–462.
[21] Liu, B., D. Wang, W. Huang, A. Yao, M. Kamitakahara, & K. Ioku, "Preparation of magnetite nanoparticles coated with silica via a sol-gel approach", Journal of the Ceramic Society of Japan. **115** (2007) 877–881.
[22] Yean, S., L. Cong, C.T. Yavuz, et al., "Effect of magnetite particle size on adsorption and desorption of arsenite and arsenate", Journal of Materials Research. **20** (2005) 3255–3264.
[23] Tamimi, A.N.J. Al, & J.F.T. Al Draji, "Synthesis and Characterization of Magnetic Iron Oxide Nanoparticles by Co-Precipitation Method at Different Conditions Ahmed", Journal of Engineering. **24** (2018) 108–128.
[24] Al-alawy, A.F., E.E. Al-abodi, & R.M. Kadhim, "Journal of Engineering", **24** (2018) 60–72.
[25] Al-deen, F.N., C. Selomulya, C. Ma, & R.L. Coppel, "Superparamagnetic Nanoparticle Delivery of DNA Vaccine", **1143** (2014) 181–194.
[26] Arvand, M., Z. Erfanifar, & M.S. Ardaki, "A New Core@Shell Silica-Coated Magnetic Molecular Imprinted Nanoparticles for Selective Detection of Sunset Yellow in Food Samples", Food Analytical Methods. **10** (2017) 2593–2606.
[27] Che, H.X., S.P. Yeap, M.S. Osman, A.L. Ahmad, & J. Lim, "Directed assembly of bifunctional silica-iron oxide nanocomposite with open shell structure", ACS Applied Materials and Interfaces.

6 (2014) 16508–16518.
[28] Kralj, S., D. Makovec, S. Čampelj, & M. Drofenik, "Producing ultra-thin silica coatings on iron-oxide nanoparticles to improve their surface reactivity", Journal of Magnetism and Magnetic Materials. **322** (2010) 1847–1853.
[29] Rajkumari, K., J. Kalita, D. Das, & L. Rokhum, "Magnetic Fe3O4@silica sulfuric acid nanoparticles promoted regioselective protection/deprotection of alcohols with dihydropyran under solvent-free conditions", RSC Advances. **7** (2017) 56559–56565.
[30] Udvardi, B., I.J. Kovács, T. Fancsik, et al., "Effects of Particle Size on the Attenuated Total Reflection Spectrum of Minerals", Applied Spectroscopy. **71** (2017) 1157–1168.
[31] Togashi, T., T. Naka, S. Asahina, K. Sato, S. Takami, & T. Adschiri, "Surfactant-Assisted One-pot Synthesis of Superparamagnetic Magnetite Nanoparticle Clusters with a Tunable Cluster Size and Sensitivity for Magnetic Field", Dalton Transactions. **40** (2011) 1073–1078.
[32] Stoia, M., R. Istratie, & C. Păcurariu, "Investigation of magnetite nanoparticles stability in air by thermal analysis and FTIR spectroscopy", Journal of Thermal Analysis and Calorimetry. **125** (2016) 1185–1198.
[33] Yeap, S.P., J. Lim, H.P. Ngang, B.S. Ooi, & A.L. Ahmad, " Role of Particle–Particle Interaction Towards Effective Interpretation of Z -Average and Particle Size Distributions from Dynamic Light Scattering (DLS) Analysis ", Journal of Nanoscience and Nanotechnology. **18** (2018) 6957–6964.
[34] Lien, Y.H., & T.M. Wu, "Preparation and characterization of thermosensitive polymers grafted onto silica-coated iron oxide nanoparticles", Journal of Colloid and Interface Science. **326** (2008) 517–521.
[35] Behera, S.S., J.K. Patra, K. Pramanik, N. Panda, & H. Thatoi, "Characterization and Evaluation of Antibacterial Activities of Chemically Synthesized Iron Oxide Nanoparticles", World Journal of Nano Science and Engineering. **02** (2012) 196–200.
[36] Maggioni, D., P. Arosio, F. Orsini, et al., "Superparamagnetic iron oxide nanoparticles stabilized by a poly(amidoamine)-rhenium complex as potential theranostic probe", Dalton Transactions. **43** (2014) 1172–1183.
[37] Carter, N., "Physical Properties of Iron Oxide Nanoparticles", Biomedical Engineering and Bioengineering Commons. **Honors Col** (2015) 210.
[38] Reddy, B.S.R., *Advances in Nanocomposites - Synthesis, Characterization and Industrial Applications*, InTech, (2011).
[39] Amaro-Gahete, J., A. Benítez, R. Otero, et al., "A comparative study of particle size distribution of graphene nanosheets synthesized by an ultrasound-assisted method", Nanomaterials. **9** (2019).
[40] Kumar, C.S.S.R., *Magnetic Characterization Techniques for Nanomaterials*, Springer-Verlag Berlin Heidelberg, (2017).
[41] Li, X., L. Liu, & F. Yang, "CFC/PVDF/GO-Fe3+membrane electrode and flow-through system improved E-Fenton performance with a low dosage of aqueous iron", Separation and Purification Technology. **193** (2018) 220–231.
[42] Ho, K.C., Y.H. teow, & A.W. mohammad, "Optimization of nanocomposite conductive membrane formulation and operating parameters for electrically-enhanced palm oil mill effluent filtration using response surface methodology", Process Safety and Environmental Protection. **126** (2019) 297–308.
[43] Li, X., & G.N. Demartino, "Aggregation effects on the magnetic properties of iron oxide colloids", Nanotechnology. (2019).
[44] Mokadem, Z., S. Mekki, S. Saïdi-Besbes, G. Agusti, A. Elaissari, & A. Derdour, "Triazole containing magnetic core-silica shell nanoparticles for Pb2+, Cu2+ and Zn2+ removal", Arabian Journal of Chemistry. **10** (2017) 1039–1051.
[45] Shnoudeh, A.J., I. Hamad, R.W. Abdo, et al., *Synthesis, Characterization, and Applications of*

Metal Nanoparticles, Elsevier Inc., (2019).